Association of chlorophyll a/c(2) complexes to photosystem I and photosystem II in the cryptophyte Rhodomonas CS24

Kereiche, Sami; Kouril, Roman; Oostergetel, Gert T.; Fusetti, Fabrizia; Boekema, Egbert J.; Doust, Alexander B.; van der Weij-de Wit, Chantal D.; Dekker, Jan P.

Published in:
Biochimica et Biophysica Acta

DOI:
10.1016/j.bbabio.2008.04.045

Publication date:
2008

Biochimica et Biophysica Acta 1777 (2008) 1122–1128

Contents lists available at ScienceDirect

Biochimica et Biophysica Acta

journal homepage: www.elsevier.com/locate/bbabio

Association of chlorophyll a/c_2 complexes to photosystem I and photosystem II in the cryptophyte *Rhodomonas* CS24

Sami Kereïche [a], Roman Kouřil [a], Gert T. Oostergetel [a], Fabrizia Fusetti [c], Egbert J. Boekema [a], Alexander B. Doust [b], Chantal D. van der Weij-de Wit [b], Jan P. Dekker [b,*]

[a] Department of Biophysical Chemistry, Groningen Biomolecular Sciences and Biotechnology Institute, University of Groningen Nijenborgh 4, 9747 AG Groningen, The Netherlands
[b] Faculty of Sciences, Division of Physics and Astronomy, VU University Amsterdam, De Boelelaan 1081, 1081 HV Amsterdam, The Netherlands
[c] Department of Biochemistry, Groningen Biomolecular Sciences and Biotechnology Institute, University of Groningen, Nijenborgh 4, 9747 AG Groningen, The Netherlands

ARTICLE INFO

Article history:
Received 29 October 2007
Received in revised form 10 April 2008
Accepted 22 April 2008
Available online 9 May 2008

Keywords:
Photosystem I
Photosystem II
Antenna protein
Rhodomonas CS24
Electron microscopy
Cryptophytes

ABSTRACT

Photosynthetic supercomplexes from the cryptophyte *Rhodomonas* CS24 were isolated by a short detergent treatment of membranes from the cryptophyte *Rhodomonas* CS24 and studied by electron microscopy and low-temperature absorption and fluorescence spectroscopy. At least three different types of supercomplexes of photosystem I (PSI) monomers and peripheral Chl a/c_2 proteins were found. The most common complexes have Chl a/c_2 complexes at both sides of the PSI core monomer and have dimensions of about 17×24 nm. The peripheral antenna in these supercomplexes shows no obvious similarities in size and/or shape with that of the PSI–LHCI supercomplexes from the green plant *Arabidopsis thaliana* and the green alga *Chlamydomonas reinhardtii*, and may be comprised of about 6–8 monomers of Chl a/c_2 light-harvesting complexes. In addition, two different types of supercomplexes of photosystem II (PSII) dimers and peripheral Chl a/c_2 proteins were found. The detected complexes consist of a PSII core dimer and three or four monomeric Chl a/c_2 proteins on one side of the PSII core at positions that in the largest complex are similar to those of Lhcb5, a monomer of the S-trimer of LHCII, Lhcb4 and Lhcb6 in green plants.

1. Introduction

Oxygenic photosynthesis occurs not only in green plants, but also in many different types of algae and cyanobacteria that live in large quantities in both salt- and freshwater habitats. All these organisms have very similar photosynthetic reaction centers in the two photosystems, i.e., photosystem I (PSI) and photosystem II (PSII). In addition they have peripheral antenna systems, which are much more diverse and can occur both intrinsically in the thylakoid membranes and extrinsically attached to these membranes. Plants have an extensive membrane-integrated light-harvesting system composed of the Lhca1-4 and Lhcb1-6 chlorophyll *a*/*b* binding proteins as main subunits, which associate in single or multiple copies to PSI and PSII into large supercomplexes [1]. These antenna proteins belong to a very large family of chlorophyll *a*/*b* binding proteins, also known as the LHC superfamily [2]. Most cyanobacteria lack such a peripheral membrane-intrinsic light-harvesting system, but have instead a large water-soluble system, the phycobilisome, which in most species is composed of multiple copies of three different types of phycobiliproteins. Phycobilisomes are associated on the stromal side of PSI and PSII, but their precise attachment sites are not known. Some types of cyanobacteria contain membrane-intrinsic antenna proteins belonging to the family of core antenna proteins, i.e., the prochlorophyte chlorophyll *a*/*b* binding proteins (Pcb's) and/or IsiA, the chlorophyll *a* binding protein that is expressed in cyanobacteria when they grow under conditions of iron limitation or other types of oxidative stress [3,4].

In this work, we focus our attention on the occurrence and structure of supramolecular associations of the two photosystems in a cryptophyte alga. Cryptophytes are eukaryotic algae that are unique because they utilize both membrane-extrinsic phycobiliproteins and membrane-intrinsic Chl a/c_2 light-harvesting proteins belonging to the LHC superfamily in their light-harvesting apparatus. The phycobiliproteins differ from those in cyanobacteria and red algae in their occurrence of only one type of phycoerythrin or phycocyanin, which are also differently organized. [5]. *Rhodomonas* CS24 contains phycoerythrin 545 (PE545), a heterodimeric ($\alpha1\beta$)($\alpha2\beta$) complex consisting of 4 polypeptides with a total mass of 60 kDa. The protein has been crystallized [6] and its structure has been solved at 0.97 Å resolution by X-ray diffraction (protein data base entry 1XG0) [7]. These phycobiliproteins are not organized into large phycobilisomes bound at the stromal side of the photosynthetic membrane, like in cyanobacteria and red algae, but they are located at the lumenal side of the membrane. Some electron microscopy studies have suggested that within the lumen the phycobilin proteins assemble into stacks or rows, although there is no real

* Corresponding author.
E-mail address: JP.Dekker@few.vu.nl (J.P. Dekker).

0005-2728/$ – see front matter © 2008 Elsevier B.V. All rights reserved.
doi:10.1016/j.bbabio.2008.04.045

consensus [5]. The chloroplast of cryptophytes is related to that of red algae [8]. Sequencing of the plastid genome of the cryptophyte *Guillardia theta* indicated the presence of PSI subunits Psa-A–E, Psa-F and Psa-I–M and the PSII subunits Psb-A–F, Psb-H–L, N T, V, and X [8], but otherwise cryptophytes have not been extensively studied genetically.

The intrinsic LHC antenna of cryptophytes appears to consist of several proteins. Originally, a *Rhodomonas* light-harvesting complex of approximately 55 kDa was detected in SDS gels, which was comprised of two polypeptide subunits of 20 and 24 kDa [9]. More recently thylakoid membranes of the cryptophyte *Rhodomonas* sp. were solubilized with the mild detergent *n*-dodecyl-β,D-maltoside (β-DM) and subjected to sucrose density gradient centrifugation [10]. The resulting gradients showed six pigment-bearing bands. Two of the bands showed characteristics of light-harvesting complexes, other bands could be attributed to PSII and PSI. Up to 10 different light-harvesting proteins could be identified, some of which are specific for PSI, others for PSII. The polypeptides of the light-harvesting complex of PSII show a higher chlorophyll *c*/*a* ratio than the antenna proteins of PSI [10]. Recently two LHC genes of *Rhodomonas* CS24 were sequenced [11] and most likely the folding of the proteins expressed by these genes is similar to that of the main light-harvesting complex of green plants (LHCII) that is structurally resolved at 2.5 Å [12,13].

Electron microscopy analysis indicates that the PSII core complex from the red alga *Porphyridium cruentum* is structurally very similar to that of cyanobacteria and the core complex of green plants [1,14]. Supramolecular associations of PSI and PSII with peripheral membrane-intrinsic antenna proteins have not yet been studied in cryptophytes and other non-green algae. In this study, we have prepared photosynthetic supercomplexes from membranes of the unicellular cryptophyte *Rhodomonas* CS24 and demonstrate by electron microscopy and single-particle image analysis that both photosystems form supercomplexes with several Chl a/c_2 proteins that are unique in size and shape and are different from those of green plants, green algae and cyanobacteria.

2. Materials and methods

2.1. Harvesting cells

Cells were pelleted by centrifugation at (4000 ×g, 15 min, 4 °C), the resulting pellet was resuspended in Hepes/KCl buffer at pH 7.8 and 1 mM of PMSF (phenylmethanesulphonylfluoride). After the addition of 0.1 mg/ml lysozyme and 30 min incubation at 4 °C, the cells were disrupted using a French Press twice at 1000 psi. After the removal of undisrupted cells the lysate was centrifuged for 10 min at 4 °C at 7000 ×*g*; the resulting pellet was discarded. The thylakoids were collected by ultra-centrifugation of the supernatant in a Centrikon T-124 A8.24 rotor (30 min, 30,000 g) and washed two times to remove water-soluble phycoerythrin antenna proteins.

2.2. Sample preparation

Thylakoid membranes were pelleted in a Eppendorf table centrifuge and resuspended in BTT buffer (Bis–Tris 20 mM pH 6.5, 20 mM NaCl, 10 mM $MgCl_2$, 1.5% taurine) at a chlorophyll concentration of 1 mg/ml, solubilized with β-DM at a final concentration of 2% during 1 min and centrifuged for 3 min at 9000 rpm in an Eppendorf table centrifuge, after which the supernatant was pushed through a 0.45 µm filter to remove large fragments. The solubilized fractions were subjected to gel filtration chromatography using two Superdex 200 HR 10/30 columns (Pharmacia) with BTT and 0.03% β-DM as mobile phase at a flow rate of 0.45 ml/min. The chromatography was performed at room temperature, while for detection a Shimadzu SPD-M10A VP diode array detector was used. Fractions of 0.3 ml each were pooled, kept at 4 °C and further analyzed. The particles were kept in darkness during the complete isolation procedure.

2.3. Spectroscopy

The isolated fractions were diluted in 20 mM Bis–Tris pH 6.5, 10 mM NaCl, 0.03% β-DM and 60% v/v glycerol to an OD at 680 nm < 0.1 cm^{-1} for fluorescence measurements and < 1 cm^{-1} for absorption measurements. A Utrex Cryostat with a gasflow temperature controller was used to vary the temperature between 6 and 280 K. Absorbance and fluorescence emission measurements were recorded on home-built spectrometers, the latter using a 0.5 m imaging spectrograph and a CCD camera (Chromex Chromcam I). Broadband excitation was provided by a tungsten halogen lamp (Oriel) and 420 nm interference filter (bandwidth ~15 nm). The spectral resolution of the detection setup was 0.3 nm. The recorded emission spectra were corrected for the wavelength sensitivity of the detection system.

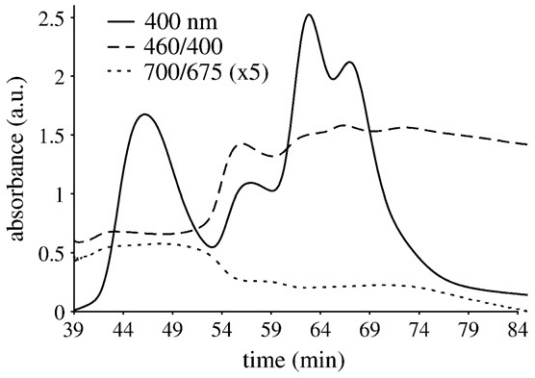

Fig. 1. FPLC chromatogram recorded at 400 nm, of the β-DM solubilized thylakoid membranes of the cryptophyte alga *Rhodomonas* CS24, obtained with the double column procedure. In the chromatogram, the ratios A460/400 and A700/675 are plotted to provide information on the relative amount of Chl *c*/*a* and red Chl *a* present, respectively. The values on the *y*-axis are the real values of these ratios.

2.4. Blue native PAGE and mass spectrometry

The fractions of the first peak eluted during size exclusion chromatography were separated by one dimension gradient (3.75–13%) blue native polyacrylamide gel electrophoresis (BN-PAGE) [15]. Subsequently, the separated protein complexes were subjected to in-gel trypsin digestion and separately analyzed by mass spectrometry using a MALDI-TOF/TOF Proteomics Analyzer (Applied Biosystems, Foster City, CA, USA), prior peptide separation on a nanoscale liquid chromatography system. Peptides with signal-to-noise level above 40 were selected for MS/MS analysis. A detailed protocol is included as Supplementary material. Protein identification was carried out using Protein Pilot (version 2.0, Applied Biosystems), searching against the *Rhodomonas salina* mitochondrial protein sequence database [16] allowing for modification by amino acid substitution. The *R. salina* protein sequences were extracted from the UniProtKB/TrEMBL database. Protein identifications with probability greater than 99.0%, based on 1 peptide identified with a probability higher than 99% or at least 2 peptides identified independently with 95% probability, were accepted.

2.5. Electron microscopy

Samples were negatively stained with 2% uranyl acetate on glow discharged carbon-coated copper grids. Electron microscopy was performed on a Philips CM120 electron microscope equipped with a LaB_6 tip operating at 120 kV. Images were recorded with a Gatan 4000 SP 4 K slow-scan CCD camera at 80,000 magnification at a pixel size (after binning the images) of 0.375 nm at the specimen level with GRACE software for semi-automated specimen selection and data acquisition [17]. Single-particle analysis of a data set of 60,000 particles was performed using GRIP (Groningen Image Processing) software, including multireference and no-reference alignments, multivariate statistical analysis, and classification, performed as described previously [18].

3. Results

3.1. Gel filtration chromatography

We solubilized thylakoid membranes from the cryptophyte *Rhodomonas* CS24 by a short treatment with the mild detergent β-DM and separated the solubilized fraction by a single gel filtration chromatography step, with the aim to keep possible supercomplexes of PSI and/or PSII with peripheral membrane-intrinsic Chl a/c_2 antenna proteins intact. With similar procedures PSII–LHCII supercomplexes from plants [18] and large PSI–LHCI supercomplexes from the green alga *Chlamydomonas* [19] were shown to stay intact.

Fig. 1 shows the chromatogram, recorded at 400 nm. Four protein peaks are discerned, at elution times of 46, 57, 63 and 67 min. The A_{460}/A_{400} ratio is representative of the Chl *c*/*a* ratio present in the different fractions. A significantly lower Chl *c* content is thus recorded for the first fraction with respect to the later fractions. The A_{700}/A_{675} ratio represents the relative amount of long-wavelength absorbing Chl *a* present in the fractions. In green plants, this ratio is normally used to

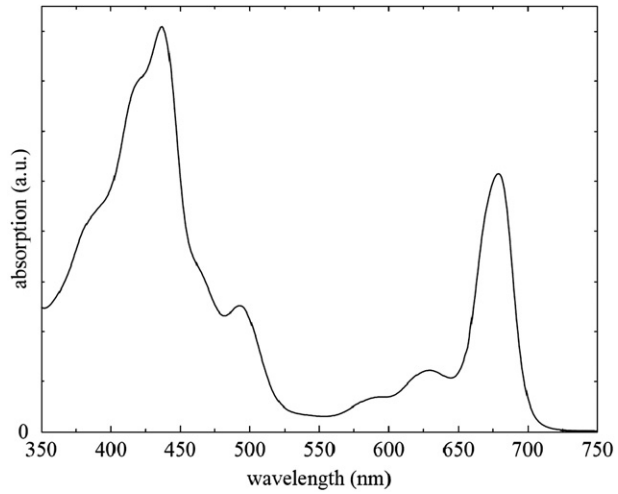

Fig. 2. Room temperature absorption spectrum of the Fraction 1 isolated from *Rhodomonas* CS24 cells.

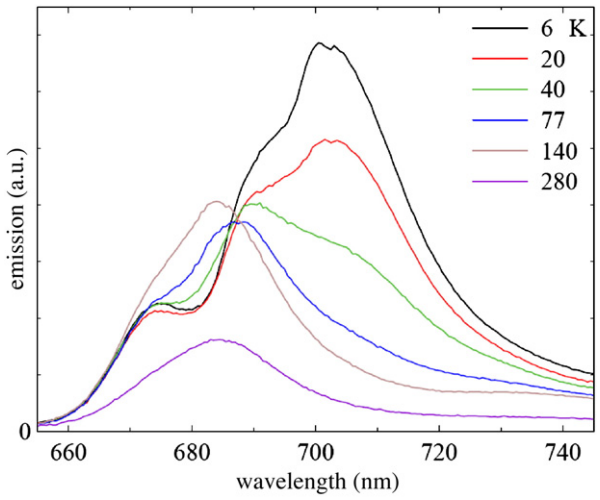

Fig. 4. Temperature dependent emission of Fraction 1 isolated from *Rhodomonas* CS24 cells. Excitation at 420 nm.

indicate the relative amount of PSI and LHCI in the fractions, since PSII and LHCII hardly absorb at 700 nm. Fig. 1 shows that this ratio is 0.1 in the first fraction and lower in all subsequent fractions. For comparison, this ratio is about 0.3 for green plant PSI supercomplexes [20]. From a time-resolved study on *Rhodomonas* CS24 intact algae it was however concluded that the amount of long-wavelength absorbing (red) pigments in PSI of *Rhodomonas* is very small [21]. Because at an elution time of 46 min only large complexes are expected to elute from the columns, we conclude that the first fraction is very likely enriched in PSI supercomplexes and may contain some PSII supercomplexes as well. We used this fraction (designated Fraction 1 in the following) for all further experiments. The later fractions, eluting at 57, 63 and 67 min, are probably enriched in Chl a/c_2 antenna units in different aggregation states, most likely monomers (67 min), dimers (63 min) and trimers or tetramers (57 min).

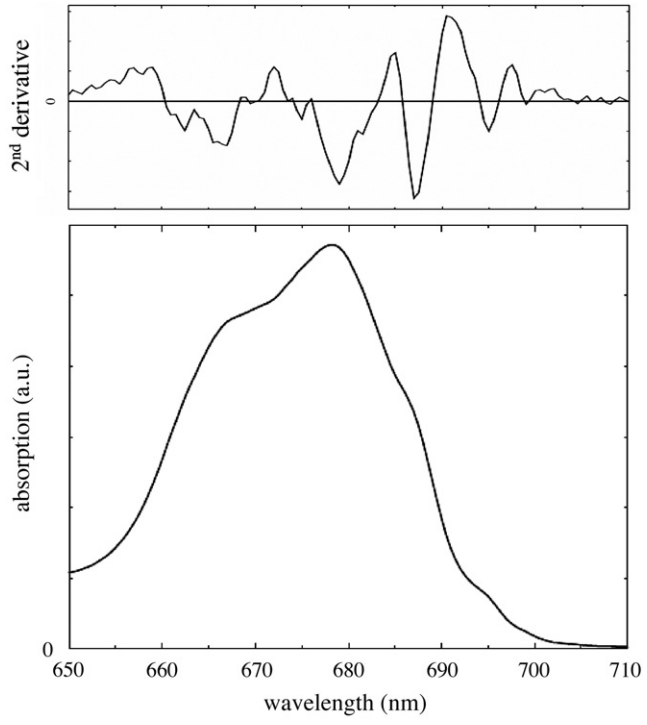

Fig. 3. 6 K absorption spectrum of Fraction 1 isolated from *Rhodomonas* CS24 cells and its second derivative.

3.2. Low temperature spectroscopy

In Fig. 2, the room temperature absorption spectrum of Fraction 1 is shown. The spectrum reveals the Chl *a* Q_Y absorption maximum at 679 nm, which is typical for PSI in green plants and cyanobacteria (see, e.g. [22]). In plants, the absorption by PSII core is known to be blue-shifted with respect to that of PSI, with absorption maximum at 674 nm [23]. In the Soret region, the Chl *a* absorption maximum is observed at 437 nm. The Soret region reveals a small contribution of Chl *c* at 467 nm. The Q_Y absorption contribution of Chl *c* around 630 nm is hidden by the broad Chl *a* Q_X absorption around that wavelength. The absorption band at 493 nm is assigned to carotenoids, which are mainly alloxanthins in *Rhodomonas* CS24.

Fig. 3 displays the 4 K absorption spectrum of Fraction 1 and its second derivative. Chl *a* absorption bands are observed at 662, 666, 675 and 679 nm as well as shoulders around 681.5, 687 and 695 nm. Note the almost complete absence of red pigments, with absorption wavelength longer than 700 nm. This spectrum resembles that of PSI core complexes from organisms without many red Chls [22,24]. The peaks at 679, 687 and 695 are typical for PSI core complexes because

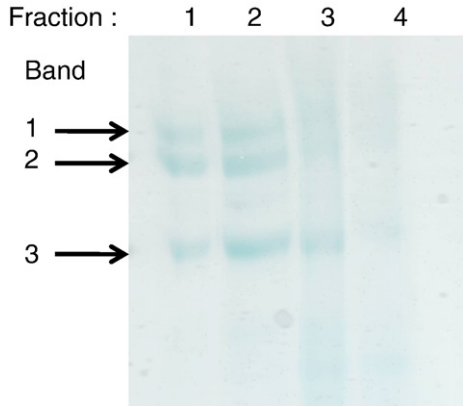

Fig. 5. Blue native PAGE of Fraction 1, which was loaded on a 13% gradient gel and stained with a colloidal Coomassie Blue stain. High-molecular mass bands (1, 2 and 3) were separately analyzed by LC-MALDI-MS/MS and all revealed the presence of PSII and PSI subunits.

Table 1
Components of PSI and PSII complexes identified by mass spectrometry

Total score	ID probability	Accession number	Protein name
23.55	99%	A6MVZ7| A6MVZ7	Photosystem I P700 chlorophyll A apoprotein A1 (Psa-A)
18.9	99%	A6MVZ6|PSAB	Photosystem I P700 chlorophyll a apoprotein A2 (PSa-B)
10	99%	A6MVZ1| A6MVZ1	Photosystem I subunit II (Psa-D)
6.1	99%	A6MW31| A6MW31	Photosystem II CP47 chlorophyll apoprotein (Psb-B)
6	99%	A6MVR3| A6MVR3	Photosystem II protein D2 (Psb-D)
6	99%	A6MVV8| A6MVV8	Photosystem I subunit XI (Psa-L)
3.26	99%	A6MVS8| A6MVS8	Photosystem I iron-sulfur center subunit VII (Psa-C)
2.44	99%	A6MVU7| A6MVU7	Photosystem I subunit III (Psa-F)
2.2	99%	A9BKV6| A9BKV6	Ranbpm

PSII usually does not have strong absorption bands at 687 and 695 nm. We conclude from this observation that PSI dominates Fraction 1, but that small amounts of PSII can not be excluded.

Fig. 4 shows the recorded emission spectra of Fraction 1 at different temperatures upon excitation at 420 nm. At 6 K, the emission maximum is observed at 702 nm and shows a shoulder at 693 and 673 nm. Since PSII emits primarily at wavelengths below 700 nm, the recorded emission maximum at 702 nm supports our assignment of Fraction 1 to be enriched in PSI, which would be caused by a 'red' Chl with about the same absorption maximum as P700. The contribution at 673 nm is seen to be rather temperature independent and is thus assigned to the presence of free Chl *a* as a result of the isolation procedure [25]. Note, that the quantum yield of the PSI fluorescence can be very small, because in PSI with only a very small number of red chlorophylls only a very small number of excitations can become trapped on these molecules, so that almost all excitations will become trapped by charge separation and will therefore give very low fluorescence quantum yields. A small PSI quantum yield also means that very minor contaminations of free Chl *a* (with very high fluorescence quantum yields) will result in relatively large contributions at 673 nm.

The emission at 702 nm is observed to largely decrease upon raising the temperature from 6 to 77 K, and conforms as reported for PSI of a cyanobacterium with a small content of red chlorophylls [22]. At 77 K, the cryptophyte PSI emission is observed to consist of a band at 687.5 nm with a shallow shoulder at wavelengths above 700 nm. There is no obvious 695 nm emission maximum in Fraction 1 at 77 K (Fig. 4), which is expected if PSII is present in significant amounts. A clear 695 nm emission band was observed in *Rhodomonas* CS24 cells at this temperature (data not shown). These data confirm that Fraction 1 consists predominantly of PSI supercomplexes and only to a small extent can it be contaminated with PSII.

3.3. Blue native PAGE and mass spectrometry analysis

The four protein fractions corresponding to the first peak obtained after size exclusion chromatography were separated by blue native poly acrylamide gel electrophoresis (BN-PAGE). The gel showed that the first two fractions were enriched in supercomplexes (Fig 5). To probe the composition of the separate complexes, the three high-molecular weight bands were excised from the BN-PAGE and separately subjected to in-gel trypsin digestion. The resulting peptides were extracted and analyzed by LC-MALDI-MS/MS. The obtained spectra were matched against the protein sequence database of the closely related organism *Rhodomonas salina*. The complete list of the matched peptides is presented in the Supplementary material (Table S1). Based on this approach the presence of Psa-A, B, C, D, F, L, as well as the presence of PSII Psb-B and D subunit, was confirmed in all three high-molecular weight bands with a confidence probability higher than 99% (Table 1). These results indicate that both PSI and PSII are present in the purified fraction (Fraction 1) which was further characterized by single-particle electron microscopy.

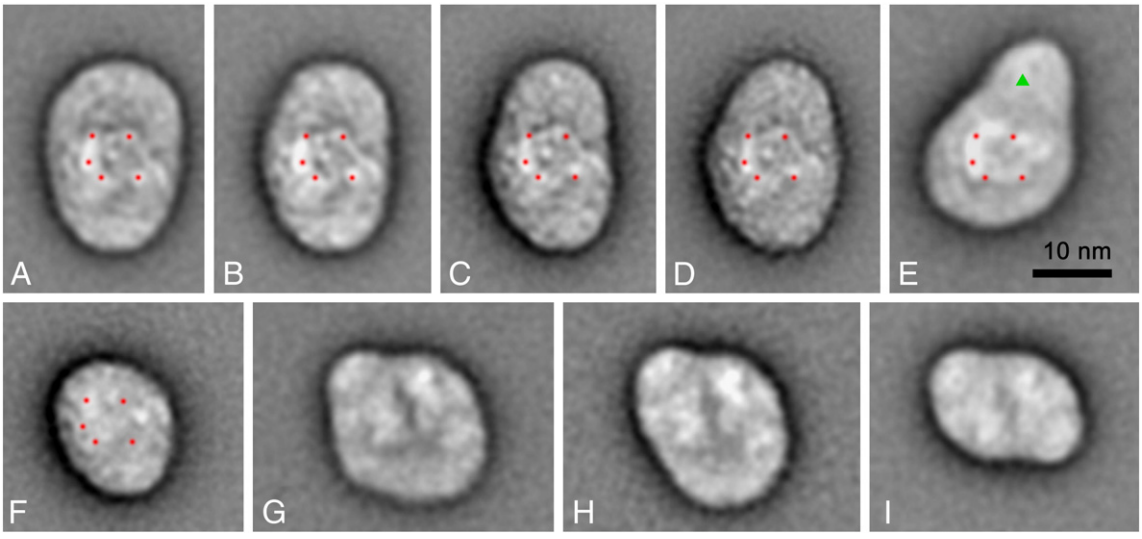

Fig. 6. Single-particle electron microscopy of PSI and PSII projections. (A,B) Projection maps of the *Rhodomonas* PSI supercomplex as in the plane of the membrane, consisting of a PSI core plus additional antenna; averages of 1024 particles, respectively; (C,D) Projection maps of the *Rhodomonas* PSI supercomplex, in slightly tilted position, averages of 2048 particles, respectively; (E) Green plant PSI–LHCII supercomplex; updated from [25]; (F) Smaller *Rhodomonas* PSI complex, consisting of a PSI core and a peripheral antenna on the lower side, average of 1024 particles; (G,H) PSII supercomplexes consisting of a dimeric core complex in the upper part and a variable peripheral antenna on the lower side; averages of 512 particles; (I) Dimeric PSII core complex, without imposed two-fold symmetry; average of 1024 particles. Red dots in frames A–F mark equivalent positions in the PSI complexes; the green triangle in frame E marks the position of the LHCII trimer in the green plant PSI supercomplex.

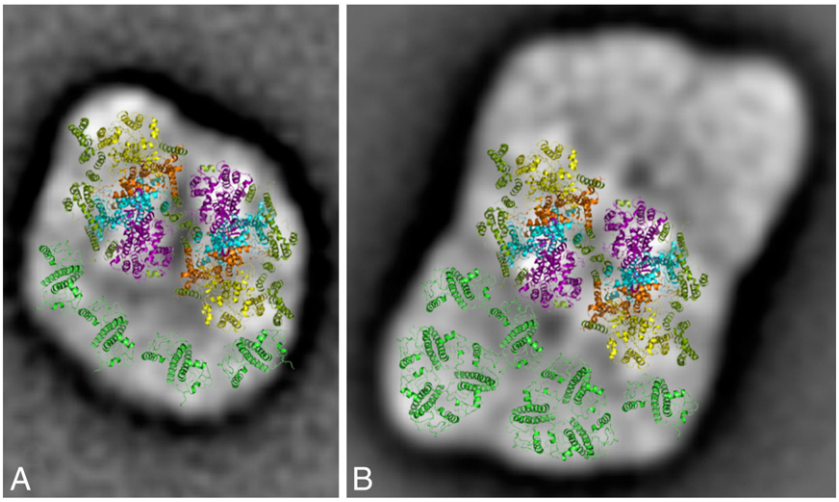

Fig. 7. Fitting of the PSII electron microscopy projection map with the high-resolution X-ray structure of dimeric cyanobacterial PSII and LHCII. (A) The map of Fig. 5G, on which the PSII structure (from [34]; protein data base entry 2AXT.pdb) and copies of monomeric plant LHCII (from [12] protein data base entry 1RWT) are superimposed. (B) Pseudo-atomic model of the $C_2S_2M_2$ PSII supercomplex, viewed from the lumenal side, derived from the EM data from *Arabidopsis thaliana*, [25] and the atomic PSII and LHCII models. CP43 (yellow), CP47 (purple), D1 (blue) and D2 (pink) are indicated.

3.4. Electron microscopy analysis

Electron microscopy was performed on freshly prepared Fraction 1. A set of 60,000 single-particle projections was collected from electron micrographs and was statistically analyzed and classified into several groups, of which the best resolved classes are shown in Fig 5. Based on similarities with 2D maps of green plant, algal and cyanobacterial PSI and PSII supercomplexes, the 2D projection maps of Fraction 1 can be clustered into two groups, of which one can be assigned to PSI (Fig. 6A–D and F) and the other to PSII complexes of variable size and shape (Fig. 6G–I).

The first group consists most likely of two different types of PSI–Chl a/c_2 supercomplexes. One is a PSI core complex with a peripheral antenna part at the lower side (Fig. 5F), the other is a core complex with additional antennas on both sides (Fig. 5A–D). The monomeric core part is similar to the PSI core from green plants, as can be seen from equivalent positions (visualized by red dots in Fig. 6A–E) in the maps of the PSI–Chl a/c_2 supercomplexes of *Rhodomonas* CS24 (Fig. 6A–D) and from the PSI–LHCII supercomplex from *A. thaliana* (Fig. 6E) [26]. The small differences between the maps of Figs. 5A, B, C, and D may have to do in part with different positions of the complexes on the EM support film. The maps of Fig. 5C and D appear smaller, probably because of a tilt away from the membrane plane. But it also seems that there is variation on the upper left side. In the map of Fig. 6A there is an additional mass at this position, which appears to be absent in the other maps, especially in the map of Fig. 6D. The maximal dimensions of the PSI–Chl a/c supercomplexes in Fig. 5A are about 17×24 nm; including the detergent boundary layer. This is significantly larger than the 17×19 nm dimensions of PSI–LHCI complex from plants, which has four Lhca proteins at the side of the PSI-F/J units [20]. The dimensions are about equal to the 17×25 nm of the PSI–LHCII supercomplex, which binds, besides the four Lhca proteins a single LHCII trimer at the PSI core site consisting of the PSI-A, -H, -L and -K subunits [26] and the PSI complex from *Chlamydomonas* which measures 19×21 nm in projection [19]. This comparison indicates that PSI of cryptophyte *Rhodomonas* CS24 may have a peripheral antenna of about 6–8 Chl a/c_2 proteins.

The second group is clearly related to PSII. Of the three obtained classes within this group, one is a "standard" dimeric PSII core complex, because its features and dimensions (19×14 nm) are very similar to those of green plants and cyanobacteria (Fig. 6I). In addition, two larger complexes were found (Fig. 6G,H), with an additional peripheral antenna that is larger in the projections of Fig. 5G than in those of Fig. 5H. The larger complexes have maximal dimensions of 17×17 and 17×16 nm. Because EM projections of membrane proteins, such as the spherical to oval-shaped *Rhodomonas* PSI projections, are difficult to assign we can not give a precise ratio between PSI and PSII complexes. The number of recognizable PSII complexes was, however, substantially lower than of PSI; in one batch it was less than a few percent, in another less than 20%. This indicates that PSI particles dominate Fraction 1, in agreement with the spectroscopy data discussed above.

4. Discussion

Statistical analysis and classification of a large set of EM projections of solubilized photosynthetic membrane proteins of *Rhodomonas* CS24 shows, for the first time in cryptophyte algae, the presence of photosynthetic supercomplexes.

The first group consists of monomeric PSI–Chl a/c_2 supercomplexes with dimensions and shapes that are significantly different from those observed for the PSI–LHCI complexes of green plants [20] and the green alga *Chlamydomonas reinhardtii* [19,27]. The crystallographic data of the green plant complex clearly shows the presence of four Lhca proteins on one side of the complex [28,29]. Most PSI–Chl a/c_2 supercomplexes (the particles shown in Fig. 6A–D) from *Rhodomonas* are significantly larger than those of green plants and have a similar surface area as the PSI–LHCI–LHCII supercomplex found in *Arabidopsis* under state 2 conditions [25]. In this complex, a total of seven Chl a/b complexes is bound to PSI: four LHCI proteins are bound at the PSI-F/J side of the complex, while one trimeric LHCII complex is bound at the side of the PSI-A, -H, -L and -K subunits. At the present resolution, the cryptophyte data do not allow an unambiguous assignment of the number of Chl a/c_2 at each side of the photosystem. The lower antenna part seems smaller and may contain 2–3 copies of Chl a/c_2 antenna complexes, whereas the upper part is bigger, especially for the particles in Fig. 6A, and may contain 4–5 copies, bringing the total number of copies to about 6–8. It is unlikely that some of the Chl a/c_2 antenna complexes appear as a (hetero)trimer attached to the PSI core, because the distance from the PSI core to the LHCII edge in the PSI–LHCII complex from *Arabidopsis* (Fig. 5E) is significantly larger than the corresponding distance in the PSI complexes from *Rhodomonas* (Fig. 6A–D). However, the lack of higher resolution does not exclude the presence of trimer(s) at the moment. We note that the gel filtration chromatography suggests the presence of three different aggregation

states of the Chl a/c_2 complexes, though details on the aggregation state of these complexes are not known.

The second group consists of a number of PSII–Chl a/c_2 supercomplexes. The core complex part of the EM projection map of *Rhodomonas* PSII does not significantly differ from its counterpart in cyanobacteria [30], green plants [1] and red algae [14]. This suggests that the major PSII subunits, including the extrinsic subunits, are present and should be structurally homologous, and also that PSII forms very similar types of dimers in all these organisms. There is no information on the extrinsic subunits, but in the genome of the distantly related red alga *C. merolae* there is a set of three extrinsic subunits PsbO, P and Q [8]. The number of the Chl *a/c* complexes associated to the core part is estimated by modeling the high-resolution structures of PSII and monomeric LHCII into the EM projection maps (Fig. 7A). This suggests that the largest particle (Fig. 6G) likely binds four copies of light-harvesting complexes on one side (Fig 7A) and that the smaller one (Fig. 6H) may bind only three copies (not shown). They flank the PSII core in about the same way as the minor antenna complexes Lhcb6, Lhcb4, one single Lhcb monomer from the LHCII S-trimer and Lhcb5 do in green plant $C_2S_2M_2$ PSII supercomplexes (Fig. 6B). The *Rhodomonas* PSII supercomplexes are also structurally similar to PSII supercomplexes of the *Prochlorococcus* species with four Pcb antenna proteins attached at each side of the PSII core dimer [31] and to those of *Prochloron didemni* which bind up to 5 Pcb complexes at each side [32]. This is remarkable, because the Pcb proteins belong to the core complex family of light-harvesting proteins, which is completely unrelated to the Cab family of light-harvesting proteins to which the Chl a/c_2 proteins of cryptophytes belong. Because the core part of *Rhodomonas* PSII is dimeric, one would expect to find particles that bind four copies of antenna complexes on both sides of the core as well. However, we could not find even small numbers of such complexes. This could hint to a conformational change in the dimer configuration, but this seems to be unlikely because the high-resolution X-ray structure of cyanobacterial PSII does not show such deviations. There exist, however, similar examples. In the mitochondrial supercomplex, consisting of dimeric Complex III (cytochrome bc_1 complex) and Complex I, there is a place for the attachment of two Complex I particles, but only one Complex I site is occupied [33]. Regardless of this uncertainty, the data unambiguously show that all Chl a/c_2 proteins bound to PSII are not trimeric. They are either monomeric, or have a dimeric arrangement similar to that of LHCI in green plants [28,29].

It is interesting to compare the PSI and PSII supercomplexes from *Rhodomonas* observed here with those from diatom algae. Diatoms are also eukaryotic algae with Chl *a/c* proteins as peripheral antennae. Recent results showed that in the diatom *Phaeodactylum tricornutum* PSI is associated with a number of Chl *a/c* proteins [35]. EM images revealed almost circular complexes with a diameter of about 21 nm, which points to a slightly larger complex than here for *Rhodomonas* and in [19] for *C. reinhardtii*. Nagao et al. were able to isolate a PSII complex with a significant number of associated Chl *a/c* proteins [36]. A structural analysis was not performed, but based on the available biochemical data a significantly larger PSII–LHC supercomplex is expected than observed here for *Rhodomonas*.

Acknowledgements

We thank Dr. W. Keegstra for his help with image processing and Henny van Roon for help with the biochemical experiments. This work has been supported by the 'Nederlandse Organisatie voor Wetenschappelijk Onderzoek (NWO)', the Netherlands Proteomics Centre, and by the Marie Curie Research Training Network Intro2 (MRTN-CT-2003-505069) of the EU. We also thank Paul Curmi and Krystyna Wilk for the cryptophyte samples, who in turn acknowledge grants from the Australian Research Council and the University of New South Wales.

Appendix A. Supplementary data

Supplementary data associated with this article can be found, in the online version, at doi:10.1016/j.bbabio.2008.04.045.

References

[1] J.P. Dekker, E.J. Boekema, Supermolecular organization of the thylakoid membrane proteins in green plants, Biochim. Biophys. Acta 1706 (2005) 12–39.
[2] B.R. Green, J.M. Anderson, W.W. Parson, in: B.R. Green, W.W. Parson (Eds.), Light-Harvesting Antennas in Photosynthesis, Kluwer, Dordrecht, 2003, pp. 1–28.
[3] R. Kouřil, A.A. Arteni, J. Lax, N. Yeremenko, S. D'Haene, M. Rögner, H.C.P. Matthijs, J.P. Dekker, E.J. Boekema, Structure and functional role of supercomplexes of IsiA and Photosystem I in cyanobacterial photosynthesis, FEBS Lett. 579 (2005) 3253–3257.
[4] J. Barber, J. Nield, J. Duncan, T.S. Bibby, in: J.H. Golbeck (Ed.), Photosystem I. The Light-Driven Plastocyanin:ferredoxin Oxidoreductase, Kluwer, Dordrecht, 2006, pp. 99–117.
[5] A.N. Macpherson, R.G. Hiller, Algae with chlorophyll c, in: B.R. Green, W.W. Parson (Eds.), Light-Harvesting Antennas in Photosynthesis, Kluwer, Dordrecht, 2003.
[6] K.E. Wilk, S.J. Harrop, L. Jankova, D. Edler, G. Keenan, F. Sharples, R.G. Hiller, P. Curmi, Evolution of a light-harvesting protein by addition of new subunits and rearrangement of conserved elements: crystal structure of a cryptophyte phycoerythrin at 1.63-angstrom resolution, Proc. Natl. Acad. Sci. U. S. A. 96 (1999) 8901–8906.
[7] A.B. Doust, C.N.J. Marai, S.J. Harrop, K.E. Wilk, P.G.M. Curmi, G.D. Scholes, Developing a structure–function model for the cryptophyte phycoerythrin 545 using ultrahigh resolution crystallography and ultrafast laser spectroscopy, J. Mol. Biol. 344 (2004) 135–153.
[8] S.E. Douglas, S.L. Penny, The plastid genome of the cryptophyte alga *Guillardia theta*: complete sequence and conserved synteny groups confirm its ancestry with red algae, J. Mol. Evol. 48 (1999) 236–244.
[9] K. Ingram, R.G. Hiller, Isolation and characterization of a major chlorophyll-a/c2 light-harvesting protein from a *Chroomonas* species (Cryptophyceae), Biochim. Biophys. Acta 722 (1983) 310–319.
[10] L. Bathke, E. Rhiel, W.E. Krumbein, J. Marquardt, Biochemical and immunochemical investigations on the light-harvesting system of the cryptophyte *Rhodomonas* sp.: evidence for a photosystem I specific antenna, Plant Biol. 1 (1999) 516–523.
[11] M.J. Broughton, C.J. Howe, R.G. Hiller, Distinctive organization of genes for light-harvesting proteins in the cryptophyte alga *Rhodomonas*, Gene 369 (2006) 72–79.
[12] Z. Liu, H. Yan, K. Wang, T. Kuang, J. Zhang, L. Gui, X. An, W. Chang, Crystal structure of spinach major light-harvesting complex at 2.72 Å resolution, Nature 428 (2004) 287–292.
[13] R. Standfuss, A.C. Terwisscha van Scheltinga, W. Kühlbrandt, Mechanisms of photoprotection and nonphotochemical quenching in pea light-harvesting complex at 2.5 Å resolution, EMBO J. 24 (2005) 919–928.
[14] L. Bumba, H. Havelkova-Dousova, M. Husak, F. Vacha, Structural characterization of photosystem II complex from red alga *Porphyridium cruentum* retaining extrinsic subunits of the oxygen-evolving complex, Eur. J. Biochem. 271 (2004) 2967–2975.
[15] H. Schägger, G. von Jagow, Blue native electrophoresis for isolation of membrane protein complexes in enzymatically active form, Anal. Biochem. 199 (1991) 223–231.
[16] H. Khan, N. Parks, C. Kozera, B.A. Curtis, B.J. Parsons, S. Bowman, J.M. Archibald, Plastid genome sequence of the cryptophyte alga *Rhodomonas salina* CCMP1319: lateral transfer of putative DNA replication machinery and a test of chromist plastid phylogeny, Mol. Biol. Evol. 24 (2007) 1832–1842.
[17] G.T. Oostergetel, W. Keegstra, A. Brisson, Automation of specimen selection and data acquisition for protein electron crystallography, Ultramicroscopy 74 (1998) 47–59.
[18] E.J. Boekema, H. van Roon, J.F.L. van Breemen, J.P. Dekker, Supramolecular organization of photosystem II and its light-harvesting antenna in partially solubilized photosystem II membranes, Eur. J. Biochem. 266 (1999) 444–452.
[19] M. Germano, A.E. Yakushevska, W. Keegstra, H.J. van Gorkom, J.P. Dekker, E.J. Boekema, Supramolecular organization of photosystem I and light-harvesting complex I in *Chlamydomonas reinhardtii*, FEBS Lett. 525 (2002) 121–125.
[20] E.J. Boekema, P.E. Jensen, E. Schlodder, J.F.L. van Breemen, H. van Roon, H.V. Scheller, J.P. Dekker, Green plant photosystem I binds light-harvesting complex I on one side of the complex, Biochemistry 40 (2001) 1029–1036.
[21] C.D. Van der Weij - de Wit, A.B. Doust, I.H.M. Van Stokkum, J.P. Dekker, K.E. Wilk, P.M.G. Curmi, G.D. Scholes, R. Van Grondelle, How energy funnels from the phycoerythrin antenna complex to photosystem I and photosystem II in cryptophyte *Rhodomonas* CS24 cells, J. Phys. Chem., B 110 (2006) 25066–25073.
[22] E.G. Andrizhiyevskaya, T.M. Schwabe, M. Germano, S. D'Haene, J. Kruip, R. van Grondelle, Spectroscopic properties of PSI–IsiA supercomplexes from the cyanobacterium *Synechococcus* PCC 7942, Biochim. Biophys. Acta 1556 (2002) 265–272.
[23] E.G. Andrizhiyevskaya, J.A. Bautista, B.A. Diner, R. van Grondelle, J.P. Dekker (2005) Energy transfer and charge separation in the photosystem II core complex studied by time-resolved fluorescence, Chapter 5, Ph.D. thesis.
[24] B. Gobets, I.H.M. van Stokkum, M. Rögner, J. Kruip, E. Schlodder, N.V. Karapetyan, J.P. Dekker, R. van Grondelle, Time-resolved fluorescence emission measurements of photosystem I particles of various cyanobacteria: a unified compartmental model, Biophys. J. 81 (2001) 407–424.
[25] S.L.S. Kwa, S. Völker, N.T. Tilly, R. van Grondelle, J.P. Dekker, Polarized site-selection spectroscopy of chlorophyll *a* in detergent, Photochem. Photobiol. 59 (1994) 219–228.
[26] R. Kouřil, A. Zygadlo, A.A. Arteni, C.D. de Wit, J.P. Dekker, P.E. Jensen, H.V. Scheller, E.J. Boekema, Structural characterization of a complex of photosystem I and

light-harvesting complex II of *Arabidopsis thaliana*, Biochemistry 44 (2005) 10935–10940.
[27] J. Kargul, J. Nield, J. Barber, Three-dimensional reconstruction of a light-harvesting complex I–photosystem I (LHCI–PSI) supercomplex from the green alga *Chlamydomonas reinhardtii* — Insights into light harvesting for PSI, J. Biol. Chem. 278 (2003) 16135–16141.
[28] A. Ben-Shem, F. Frolow, N. Nelson, Crystal structure of plant photosystem I, Nature 426 (2003) 630–635.
[29] A. Amunts, O. Drory, N. Nelson, The structure of a plant photosystem I supercomplex at 3.4 angstrom resolution, Nature 447 (2007) 58–63.
[30] A.A. Arteni, M. Nowaczyk, J. Lax, R. Kouril, M. Rögner, E.J. Boekema, Single particle electron microscopy in combination with mass spectrometry to investigate novel complexes of membrane proteins, J. Struct. Biol. 149 (2005) 325–331.
[31] T.S. Bibby, I. Mary, J. Nield, F. Partensky, J. Barber, Low-light-adapted *Prochlorococcus* species possess specific antennae for each photosystem, Nature 424 (2003) 1051–1054.
[32] T.S. Bibby, J. Nield, M. Chen, A.W. Larkum, J. Barber, Structure of a photosystem II supercomplex isolated from *Prochloron didemni* retaining its chlorophyll a/b light-harvesting system, Proc. Natl. Acad. Sci. U. S. A. 100 (2003) 9050–9054.
[33] N.V. Dudkina, H. Eubel, W. Keegstra, E.J. Boekema, H.-P. Braun, Structure of a mitochondrial supercomplex formed by respiratory chain complexes I and III, Proc. Natl. Acad. Sci. U. S. A. 102 (2005) 3225–3229.
[34] B. Loll, J. Kern, W. Saenger, A. Zouni, J. Biesiadka, Towards complete cofactor arrangement in the 3.0 Å resolution structure of photosystem, Nature 438 (2005) 1040–1044.
[35] T. Veith, C. Büchel, The monomeric photosystem I-complex of the diatom *Phaeodactylum tricornutum* binds specific fucoxanthin chlorophyll proteins (FCPs) as light-harvesting complexes, Biochim. Biophys. Acta 1767 (2007) 1428–1435.
[36] R. Nagao, A. Ishii, O. Tada, T. Suzuki, N. Dohmae, A. Okumura, M. Iwai, T. Takahashi, Y. Kashino, I. Enami, Isolation and characterization of oxygen-evolving thylakoid membranes and photosystem II particles from a marine diatom *Chaetoceros gracilis*, Biochim. Biophys. Acta 1767 (2007) 1353–1362.